USGS Award No. 06HQGR0131

DEEP SHEAR WAVE VELOCITY PROFILES OF MISSISSIPPI EMBAYMENT SEDIMENTS DETERMINED FROM SURFACE WAVE MEASUREMENTS

Brent L. Rosenblad, Ph.D.
University of Missouri
Department of Civil and Environmental Engineering
E2509 Lafferre Hall
Columbia, MO 65211
Tel: 573-884-3736
Fax: 573-882-4784
rosenbladb@missouri.edu

Research supported by the U.S. Geological Survey (USGS), Department of the Interior, under USGS award number 06HQGR0131. The views and conclusions contained in this document are those of the authors and should not be interpreted as necessarily representing the official policies, either expressed or implied, of the U.S. Government.

ABSTRACT

The deep soils of the Mississippi embayment in the central United States will have a significant influence on earthquake ground motions generated in the New Madrid seismic zone. The dynamic properties of these soils, which extend to depths of over 1000 meters in some areas, are poorly characterized at depths below 60 to 100 meters. This study presents shear wave velocity (V_s) profiles determined from surface wave measurements performed at six sites located in Arkansas, Tennessee, and Missouri. These measurements were performed using the low-frequency field vibrator ('Liquidator') developed as part of the National Science Foundation's (NSF) Network for Earthquake Engineering Simulation (NEES) program. Shear wave velocity profiles were developed to depths of approximately 220 meters. The V_s profiles developed for the six measurement sites, along with profiles developed at five sites from a previous study, were used to study the variability of V_s profiles in the embayment and develop relationships between V_s and soil lithology. The average V_s profile derived from the eleven surface wave measurements compared well with V_s reference profiles that have been developed for the Mississippi embayment and used in recent site response studies of the region. The observed variability of the V_s profiles from site-to-site was associated with changes in soil lithology. Relationships between soil lithology and V_s were consistent with past shallow studies and provided information to greater depths.

INTRODUCTION

The upper Mississippi embayment region of the central United States spans the states of Missouri, Kentucky, Arkansas, and Tennessee, and overlies the New Madrid seismic zone (NMSZ). Sediments in this region extend to depths of up to 1000 meters in some locations. The presence of these deep deposits will influence the amplitude and frequency content of future earthquake ground motion. In order to better predict the ground motions and design structures that will perform safely in a large seismic event, a reliable model of the deep sediment dynamic properties, particularly the shear wave velocity (V_s) profile is needed. Non-intrusive surface wave methods have been demonstrated to be an effective means to determine in-situ V_s values for site response studies (Bay 2003; Brown et al. 2000; Brown et al. 2002).

The penetration depth of surface wave measurements depends on the ability to excite low-frequency surface waves. Impact sources typically produce maximum penetration depths of approximately 30 to 50 meters. Even with the use of conventional Vibroseis equipment, the depth of penetration is usually limited to about 75 meters or less at most soil sites. Recently, a unique low-frequency vibrator has been developed at the University of Texas at Austin as part of the Network for Earthquake Engineering Simulation (NEES) project. The low-frequency limit of this equipment extends over two octaves below the range of a conventional Vibroseis and should provide V_s profiles that penetrate three or four times as deep as those produced with conventional Vibroseis equipment.

The motivation for this study is the current lack of deep V_s measurements throughout the upper Mississippi Embayment. The vast majority of V_s studies in the Mississippi embayment have been confined to the top 60 meters, with most site classification studies focused on determining V_s values in the top 30 meters of the soil deposits. Studies by Park and Hashash (2005) have demonstrated the important effect deep sediments will have on the amplitude and frequency content of ground motions. A common reference V_s profile that has been used in site response studies is based on deep soil information derived from limited data and assumed values of variability for deeper deposits (Romero and Rix, 2001).

The primary objective of this research project is to non-intrusively characterize the V_s structure of upper Mississippi embayment sediments to depths of 200 to 250 meters at six deep soil sites. This data fills an existing gap in knowledge of the small-strain V_s structure and spatial variability of the Mississippi embayment sediments. The second objective is to use the results of this work, in combination with five deep soil profiles developed from a previous study, to develop relationships between V_s and soil lithology in the upper Mississippi Embayment. This report presents the results obtained for these two research objectives.

OVERVIEW OF THE MISSISSIPPI EMBAYMENT GEOLOGY

The general stratigraphy for the New Madrid seismic zone, as developed by Van Arsdale and TenBrink (2000), is presented in Figure 1. The profile shown extends to bedrock. The profile depth achieved in this study from the surface wave velocity measurements generally did not extend beyond the base of the Eocene Claiborne group. The formations sampled in this study are discussed below.

The Eocene Claiborne Group is divided into the Memphis Sand, the Cook Mountain Formation, and the Cockfield Formation. The Memphis Sand is fluvial/deltaic sand that ranges from approximately 225-meters thick below Shelby County, Tennessee, thinning to about 110-meters thick below New Madrid, Missouri. The Memphis Sand also has subordinate lenses or beds of clay and silt (Van Arsdale and TenBrink, 2000) and is the major aquifer providing water to Memphis. The top of the Memphis Sand layer as well as the bottom boundary, or start of the Wilcox Group, are defined as hydrologic boundaries. The layer is part of the middle Claiborne aquifer, as well as the lower Claiborne-upper Wilcox aquifer system (Parks and Carmichael, 1990). Above the Memphis Sand, the Cook Mountain Formation is a clay and silt fluvial /deltaic unit with minor sand lenses and lignite beds. The Cockfield Formation, located over the Cook Mountain Formation, is a fluvial/deltaic silt and clay interbedded with sand and lignite beds. These two formations have a combined thickness of about 65 meters under Shelby County and 30 meters under sites in southern Missouri (Van Arsdale and TenBrink, 2000).

The Jackson Formation is fluvial/deltaic silty sand interbedded with clayey silt and lignite. The Jackson Formation becomes thicker in the northern portions of the embayment, increasing from about 15 meters under Shelby County in Memphis, Tennessee to approximately 40 meters beneath New Madrid, Missouri. The Jackson formation has a variable thickness throughout the embayment because its upper contact is an unconformity overlain by Quatenary Mississippi River alluvium within the valley and by the Pliocene-Pleistocene Lafayette Formation (Upland Complex Gravel) on the bluffs east of the Mississippi River (Van Arsdale and TenBrink, 2000). The Mississippi River sediments, which consist of basal sandy gravel overlain by sands and capped by silts and clays, have a thickness of approximately 50 meters (Saucier, 1994).

The near-surface lithology is different between the west and east sides of the Mississippi River (as shown in Fig. 2). On the eastern side of the bluffs the near-surface stratigraphy consists of the Upland Gravel and the overlying Pleistocene loess whereas on the western side of the Mississippi River bluffs the surface stratigraphy consists of Mississippi River Pleistocene (traces) and Holocene alluvium (Van Arsdale and TenBrink, 2000).

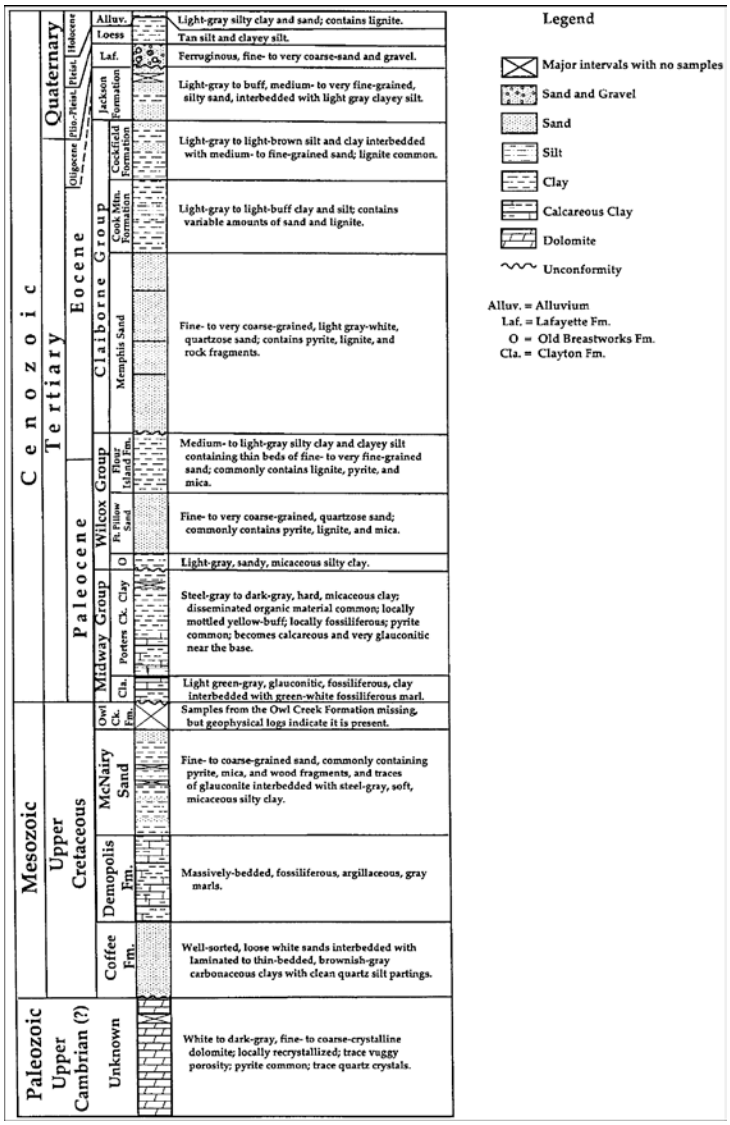

Figure 1 Geologic column for the New Madrid seismic zone (Van Arsdale and TenBrink 2000)

SITE SELECTION

As part of this USGS NEHRP project, surface wave velocity measurements were performed in May, 2007 at six locations in Missouri, Arkansas, and Tennessee. These six locations are designated as Sites 6 through 11 in Fig. 2. In May, 2006 measurements were performed at five other sites (designated as Site 1 through 5 in Fig. 2) as part of a National Science Foundation (NSF) sponsored project on surface wave methods for deep shear wave velocity profiling, performed by the project investigator. The results from this 2006 study are included in the analyses performed in this study to characterize V_S variability and correlations with lithology in the Mississippi embayment. Table 1 presents the coordinates of each of the eleven sites, as well as the estimated depth to bedrock.

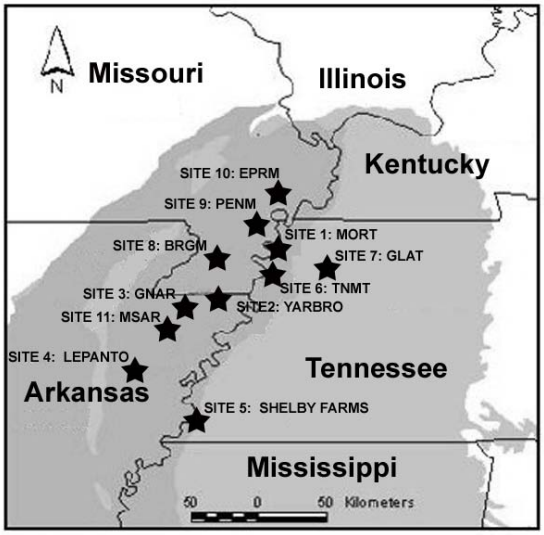

Figure 2 Map of upper Mississippi embayment showing Holocene-age deposits (dark gray), Pleistocene-age deposits (light gray), and measurement locations (modified from Romero and Rix 2001).

Table 1 Site Coordinates and Estimated Depth to Bedrock (Δ denotes CERI Station)

Site No.	Site Name	Site Coordinates		Depth to Bedrock
		Latitude (N)	Longitude (W)	m
1	MORT$^{\Delta}$	36.324	89.566	703
2	YARBRO	35.981	89.915	820
3	GNAR$^{\Delta}$	35.960	90.016	783
4	LEPANTO	35.614	90.413	794
5	SHELBY	35.136	89.843	840
6	TNMT$^{\Delta}$	36.166	89.579	783
7	GLAT$^{\Delta}$	36.269	89.288	751
8	BRGM$^{\Delta}$	36.205	89.859	714
9	PENM$^{\Delta}$	36.450	89.628	586
10	EPRM$^{\Delta}$	36.717	89.358	451
11	MSAR$^{\Delta}$	35.784	90.147	847

Sites were chosen based on multiple criteria. First, the large field vibrator ("Liquidator") used in this study had to be able to access the site and operate safely without affecting nearby structures. Secondly, the site needed to have a flat linear stretch of open land in excess of 600 meters in length to allow for deployment of the sensors. Also for sites that met the previous criteria, permission had to be obtained from the local landowner to access the site. When possible, sites were chosen adjacent to seismic stations operated by the Center for Earthquake Research and Information (CERI) at the University of Memphis. Also, sites near the location of previous research studies were considered. Lastly, it was desired to distribute the sites around the Mississippi embayment to sample variable sediment conditions and depths to bedrock.

The lithology at each site was established from a detailed structural contour map of formation tops developed by Prof. Roy Van Arsdale and his students at the University of Memphis. The map was developed from geotechnical and geophysical well logs as well as seismic reflection lines performed in the embayment. This structural map provided interpolated values of formation tops of the silt/clay, sand, and gravel layers in the Mississippi River alluvium; as well as the estimated top of the Upper Claiborne unit (Jackson, Cockfield and Cook Mountain Formations) and the top of the Memphis Sand Formation. The unit tops within the alluvium and the top of the Upper Claiborne unit were based on well information that was typically within 0.5 to 1.5 km of each site, whereas the depth of the Memphis Sand was based on wells that were typically within 4 to 9 km of the measurement sites.

SURFACE WAVE DATA COLLECTION AND ANALYSIS

Overview of the SASW Method

This research utilized the Spectral-Analysis-of-Surface-Waves (SASW) method in the data collection and analysis procedures. The SASW method is one of several methods that use Rayleigh waves to estimate V_s profiles. The primary advantage to the method is that it is non-intrusive, with the source and receivers placed directly on the ground surface. It is lower in cost as compared to conventional borehole methods, and allows for the characterization of soils that cannot be easily sampled. The method is based on the frequency-dependent penetration of surface wave energy. Surface waves with different wavelengths reach different layers of the system producing a variation of surface wave velocity with frequency in a system with depth-dependent velocities (Stokoe et al. 1988). The receiver spacing and source characteristics are varied depending on the profile depth of interest. To measure near-surface layers, a short receiver spacing with a high-frequency source is used, whereas to sample deeper deposits a longer receiver spacing is required with a low-frequency source.

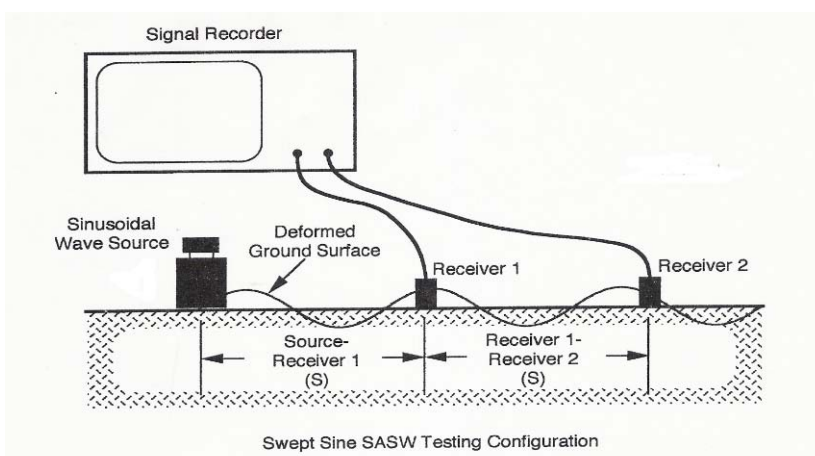

Figure 3 SASW testing configuration using a swept-sine excitation (from Rix and Stokoe 1989)

The SASW measurement may be performed using an impulse, swept-sinusoidal or random-noise source at the ground surface. Vertically oriented receivers are placed on the surface, which record the vertical component of surface motions produced from surface waves. The general setup is shown in Figure 3. In most cases equal source-to-first-receiver and receiver-to-receiver spacing is used, as shown in Figure 3. The receiver data is then digitized and recorded by a dynamic signal analyzer. A Fast Fourier Transform algorithm is used to calculate the wrapped phase difference, $\phi(f)$, between receiver pairs. The phase plot is manually unwrapped and the travel time, $t(f)$, between receivers is computed at each frequency by:

$$t(f) = \frac{\phi(f)}{360 \cdot f} \tag{1}$$

where ϕ is the unwrapped phase difference in degrees and (f) is the frequency in cycles per second. The distance between receivers (S) is known, so the wave velocity (V_R) is calculated using:

$$V_R = \frac{S}{t(f)} \tag{2}$$

The corresponding surface wavelength (λ_R) is determined using:

$$\lambda_R = \frac{V_R}{f} \tag{3}$$

These calculations are performed for each frequency with the resulting data plotted as velocity versus frequency (or wavelength), termed an individual dispersion curve (Stokoe et al., 1994). This procedure is repeated for all receiver pairs, producing multiple dispersion curves with overlapping sections between adjacent receiver pairs. The multiple dispersions curves are then combined to form a composite experimental (field) dispersion curve spanning the wavelengths (or frequency) of interest. The dispersion curve is an "apparent" velocity dispersion curve and may contain contributions from body wave and multiple surface wave modes. An inversion procedure is then used to determine the V_s profile that provides a matching theoretical dispersion curve to the experimental dispersion curve. The V_s profile that produces a theoretical dispersion curve most closely matching the experimental dispersion curve is presented as the V_s profile for the site.

Field Equipment and Instrumentation

All receivers used in this study were 1-Hz geophones manufactured by Mark Products, Inc. (L-4 seismometers). These geophones have a flat response over a range of approximately 2 Hz to 100 Hz. Each geophone was calibrated in the lab at the Network for Earthquake Engineering Simulation (NEES) facility at the University of Texas at Austin and pairs that were well matched in phase were used for low-frequency measurements.

For high-frequency, short-wavelength measurements (20-meters and less) an instrumented sledgehammer was used to excite the surface wave energy. The low frequency, long-wavelength measurements were performed using the NEES mobile field shaker known as

Liquidator (Stokoe et al. 2004). The vibrator, shown in Figure 4, was developed as part of the NSF-supported NEES program. This source is able to provide much higher output than a conventional Vibroseis source at frequencies below 4 Hz and can operate to frequencies of less than 1 Hz. The truck weighs 31,750 kg (70,000 lbs) and is 9.75 m (32 ft) long by 2.45 m (8 ft) wide. The truck has two vibration orientations, horizontally or vertically, but was set up to shake vertically for this study. The reaction mass is a 5,900-kg (13,000-lb) block of steel. The peak-to-peak stroke of the reaction mass is 0.4 m (16 in.), with the truck being able to produce a peak force of 89 kN (20,000 lbs). Liquidator can operate at frequencies from 80 Hz to less than 0.5 Hz.

Figure 4 Photograph of low-frequency mobile shaker "Liquidator" developed as part of the Network for Earthquake Engineering Simulation (NEES) program.

Data Collection

Data was collected using receiver pairs with spacing that ranged from as small as 2 m, using the hammer source, to 300 m using the NEES vibrator (Bailey 2008). Typically 7 to 10 receiver pairs were used to construct the dispersion curve. Each receiver location was surveyed in using a total station. After the locations were surveyed, the receivers were buried and leveled on site, as shown in Fig. 5. Due to the high temperatures in the field, excessive geophone temperatures that could impact the geophone performance were controlled by surrounding the geophones with cold packs and insulation. The temperature of each geophone was monitored throughout the testing using an infrared thermometer to assure that they were within their operational limits.

Figure 5 Photograph of 1-Hz geophone after placement in the ground and leveled.

Data was collected using a VXI-Technology, 48-channel dynamic signal analyzer for the sites measured in 2006, and a Data Physics dynamic signal analyzer for the sites measured in 2007. The source output of the dynamic signal analyzer was used to control the vibration frequency and amplitude of the source. The SASW measurements were performed in stepped-sine mode. A frequency range from about 0.7 Hz to 12 Hz was typically used at each site. The number of averages at each frequency ranged from 5 to 20 and the integration time was typically 20 cycles.

Data Processing

The stepped-sine measurements allowed for calculation of the cross-power spectra which provides the phase difference between each receiver pair. The signal is transformed into the frequency domain *(X(f)* and *Y(f))* and the power spectra *(G_{XX}* and *G_{YY})*, cross spectrum *(G_{XY})*, wrapped phase *($\phi(f)$)*, and the coherence function *(γ^2)* are calculated from:

$$G_{XX} = X^*(f)X(f) \tag{4}$$

$$G_{YY} = Y^*(f)Y(f) \tag{5}$$

$$G_{XY} = X^*(f)Y(f) \tag{6}$$

$$\phi(f) = \arctan\frac{\mathrm{Im}(G_{XY})}{\mathrm{Re}(G_{XY})} \tag{7}$$

$$\gamma^2 = \frac{G_{XY}G_{XY}^*}{G_{XX}G_{YY}} \tag{8}$$

where (*) represents the complex conjugate of the quantity, Im signifies the imaginary part of the expression, and Re signifies the real part of the expression.

The phase of the cross spectrum and the coherence function are key spectral quantities in SASW measurements. The coherence function indicates the quality of the measurements. A coherence value near one indicates a high signal-to-noise ratio with values going towards zero as the data quality decreases. The phase of the cross power spectrum represents the wrapped phase difference (lead or lag of 180°) between the two receivers. One set of spectral functions is measured for each receiver pair spacing.

Figure 6 shows an example of a wrapped phase spectrum and coherence function, recorded using a receiver spacing of 300 meters at Site 1. To avoid near-field effects, wavelengths of greater than twice the source-to-receiver spacing (phase of 180 º or less) are not included in the analysis. This means that for a maximum receiver spacing of 300 m, the longest wavelength that is used is 600 m. Figure 7a shows an example of an experimental dispersion curve created from seven receiver pairs with spacing ranging from 2 to 300 m.

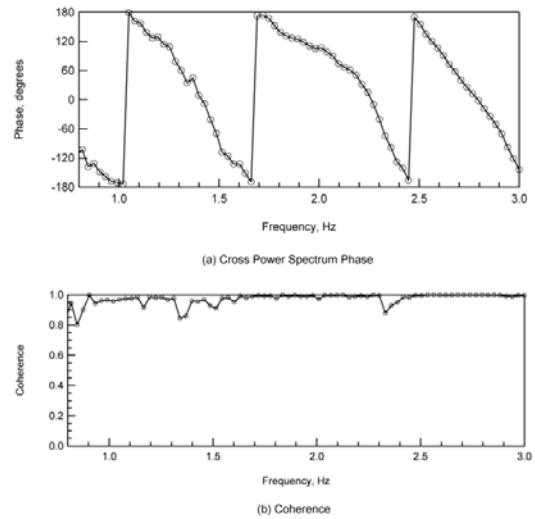

Figure 6 Cross power spectrum and coherence plot from 300 meter receiver spacing at Site 1 (Rosenblad et al. 2007).

Data Inversion

This study utilized the surface wave inversion program WinSASW 2.3.1 created at the University of Texas at Austin, to develop V_s profiles from the measured dispersion curves. An automated array inversion technique described by Joh (1996) and implemented in WinSASW2 was used to develop the V_s profiles for the eleven site locations. The array inversion technique involves calculating individual theoretical dispersion curves for each receiver pair location used in the experimental measurements using a one-dimensional layered model. The mismatch between the experimental and theoretical dispersion curves is calculated and the model parameters are updated using the sensitivity matrix calculated from the forward equation. The forward equation calculated in WinSASW2 uses the stiffness matrix approach (Kausel and Roesset 1981) and requires input of: layer thickness, V_s, Poisson's ratio (or compression wave velocity [V_p]), mass density, and material damping ratio.

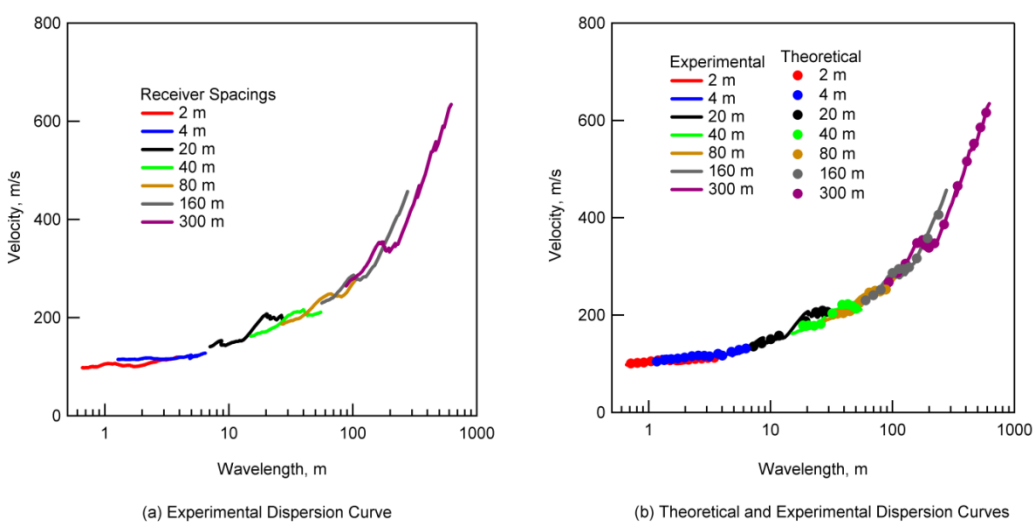

Figure 7 (a) Experimental dispersion curve from Site 1 and (b) theoretical and experimental dispersion curve fit after completion of inversion analysis (Rosenblad et al. 2007).

The parameters used in this study were as follows. For soils above the water table (depth of 4 m or less), a Poisson's ratio value of 0.25 was assumed. Below the water table, V_p of 1600 m/s was assumed for soils with V_s of 650 m/s or less. The V_p was increased to 1800 m/s for soils with V_s greater than 650 m/s. These values are consistent (within 10%) with V_p measurements over a similar depth range obtained from well logs in the embayment (Cramer et al. 2004). Mass density values of 1,900 kg/m^3 and material damping ratios of 2% were assumed for all soil layers. Mass density values are consistent (within 5%) with values used in other studies (Romero and Rix 2001; Cramer 2006) and damping values are consistent with those reported by Chen et al. (1994).

The inversion procedure implemented in WinSASW2 is a maximum likelihood approach that consists of two general steps. First, a starting V_s model is developed from the measured dispersion data. This procedure involves creating a layered profile with the same number of layers as there are points in the experimental dispersion curve. The thickness of each layer is determined based on the wavelength of the given dispersion data point and an assumed depth-to-wavelength factor, α. The V_s of the layers are determined one-by-one starting from the top layer and working down. The first layer is assumed to be a single layer system and the stiffness matrix for this system is assembled. The V_s is initially assumed to be the same as the phase velocity and is then varied to make the determinant of the stiffness matrix zero. This procedure is repeated for the second point using a two-layer system and continued on for all of the data points. From this preliminary profile, a starting profile is determined using the profile layering information input into the program and averaging the velocity values in these profile layers. The forward model is then solved using this starting model and the RMS error calculated. The entire process is repeated for a range of α values (typically five values in the range of 0.4 to 0.8 were used) in order to find the best-fitting starting model.

Once the best starting model is found the inversion procedure is applied. The inversion engine consists of the calculation of the misfit between experimental and theoretical dispersion curves and updating the model parameters. The approach developed by Joh (1996) requires estimates of the standard deviations for the data values and the model values to provide stability to the inversion process. For this study, a value of 5% of the data and model values was used for the estimated standard deviation. Details of the inversion approach are provided in Joh (1996).

The generic profile layering used in this study was created using thicker layers at greater depths to account for the decreased sensitivity to layer thickness with depth. Layer thickness was increased from less than 1 m at the surface to over 50 m at a depth of 200 m. No *a priori* information on stratigraphy was used to develop the profile layering. The initial profile layering extended to a depth of 400 m (two-thirds of the maximum wavelength). Several iterations of the inversion procedure were performed until the best fit was achieved between the experimental and theoretical dispersion curves as indicated by the root-mean-square (RMS) error. Figure 7b presents the experimental and matching theoretical dispersion curves developed for the data shown in Figure 7a. The ability of the array inversion approach to fit the variations in the individual dispersion curves using a single one-dimensional profile can be observed in Fig. 7b.

Once a theoretical dispersion curve was matched with the experimental dispersion curve a depth resolution analysis was performed. For this study the depth of resolution of each profile was determined from a manual sensitivity study of the response of the theoretical dispersion curve to changes in the V_s of the deepest layer. This procedure involved changing the velocity of

the deepest layer by 25% and observing the change in the phase velocity at the longest wavelength. If no appreciable change was observed in the dispersion curve, the lowest layer was removed and the half-space velocity was assigned to the value of the next higher layer. The procedure was repeated until a change of approximately 5% was observed in the theoretical dispersion curve at the longest wavelength. The sensitivity of each layer to the profile was indicated by increasing and decreasing the V_s value until a 10% change in RMS error was observed. An example of the V_s profile produced after the resolution and sensitivity analysis were performed is presented in Fig. 8. The bars on each layer represent the layer sensitivity. The inversion analysis described here was performed without any knowledge of the soil lithology at the site. After information on the lithology was obtained for each site, a second inversion analysis was performed using thicker layers and layer boundaries that were consistent with the expected depths and thickness of soil formations, as discussed later in this report.

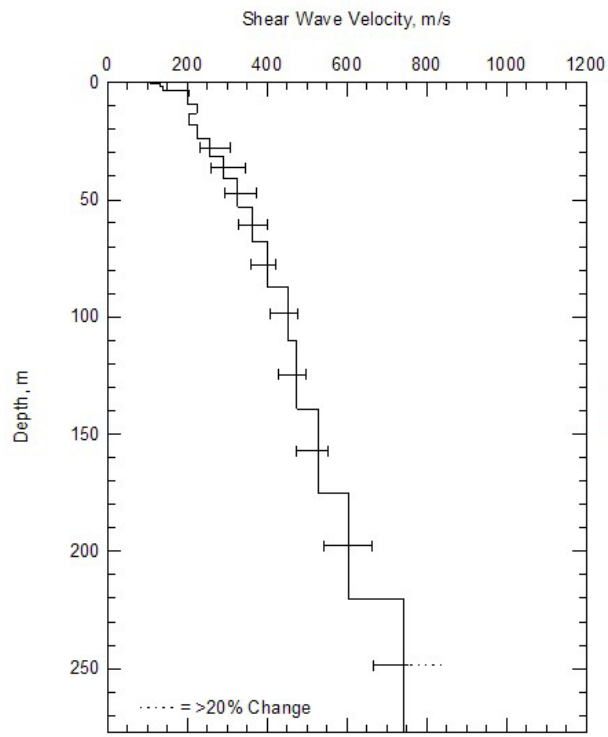

Figure 8 Shear wave velocity profile determined from SASW measurements at Site 1. Bars indicate change in V_S value to cause a 10% change in RMS values between experimental and theoretical dispersion curves.

RESULTS and DISCUSSION

SASW Analysis with Generic Profile Layering

For each of the eleven sites, a V_s profile was developed using a generic profile layering. The generic layering was developed with no *a priori* knowledge of the lithologic profile at the site. The purpose of this was to see how well changes in V_s coming from the general surface wave inversion procedure corresponded with the estimated depth of changes in lithology. Later, thicker layering with boundaries consistent with estimated formation depths was used to provide

better estimates of the average V_s in different soil formations. The data were processed and the inversion procedure was performed as discussed above. Figure 9 shows the profiles that were developed at each site and the estimated lithology for each location, provided by Prof. Roy Van Arsdale from the University of Memphis. The V_s profiles are presented in tabular form in the Appendix to this report.

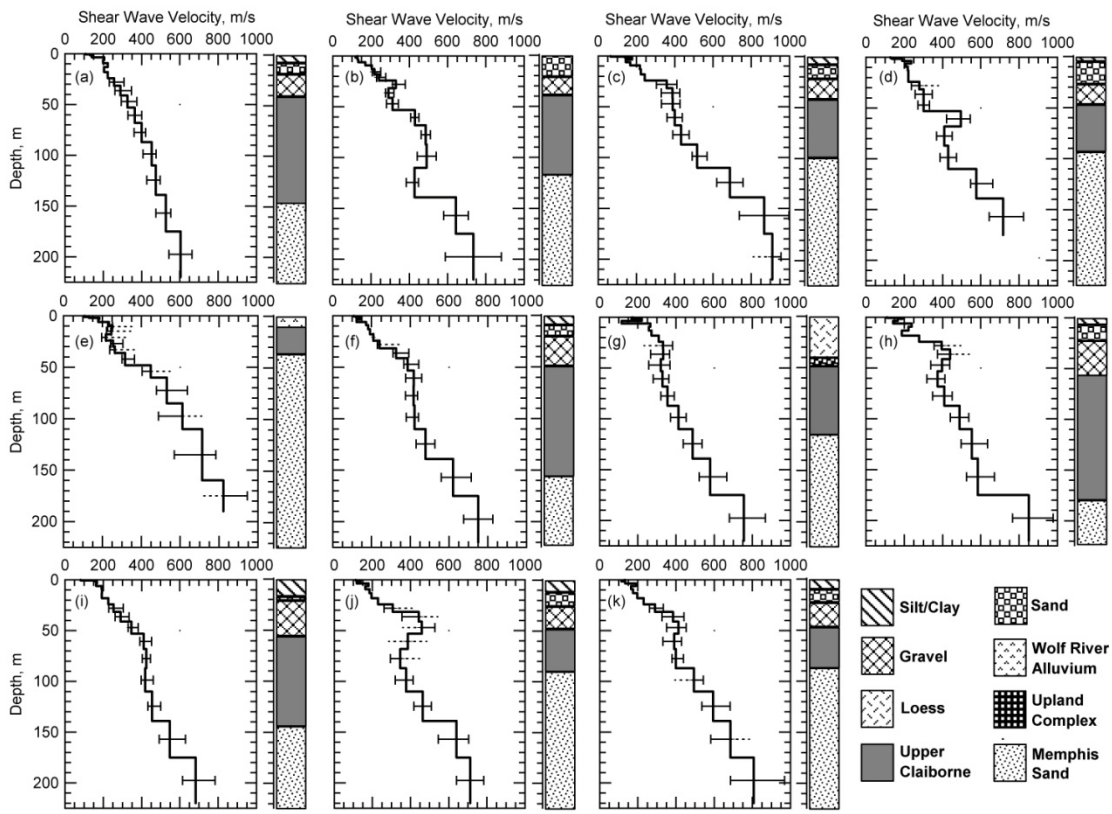

Figure 9 Shear wave velocity profiles at Sites 1 through 11 determined from SASW analyses using a generic profile layering in the inversion. Estimated soil lithology at each site is also shown.

The V_S profiles developed at these eleven sites generally show three regions of V_S values consisting of: (1) a high-gradient, low-velocity near-surface region (2) an intermediate region with shear wave velocities of about 400 to 450 m/s, and (3) a high-velocity region at depth with velocities increasing to 600 to 800 m/s. Average shear wave velocities in the top 30 m were calculated using:

$$\overline{V}_{S30} = \frac{\sum_{1}^{n} d_i}{\sum_{1}^{n} \frac{d_i}{V_{si}}} \qquad (2)$$

where, d_i is the thickness of layer *i*, $\overline{V}_{Si}$ is the shear wave velocity of layer *i*, and $\overline{V}_{S30}$ is the average shear wave velocity in the top 30 m. Figure 10 presents a comparison of the V_{S30} values, which ranged from 180 m/s to 224 m/s at the alluvial sites, while the upland site with older near-

surface loess deposits (Site 7) had a slightly higher value of 247 m/s. In all cases the sites are classified as site class D according to the IBC code.

Below the soft, near-surface deposits, the shear wave velocity profiles generally show a distinct transition to a fairly uniform shear wave velocity value of about 400 m/s. When compared with the estimated soil profiles at each site, it is apparent that this velocity zone is associated with the Upper Claiborne unit (Jackson, Cockfield and Cook Mountain Formations). For example, at Sites 1, 6, and 9, where the Upper Claiborne unit extends to depths of about 150 m, the shear wave velocity profile flattens out and remains below about 500 m/s, while at sites where these deposits are much thinner (3, 4, 5, and 11) the velocities at depths of 100 to 150 m are well over 600 m/s. The velocity transition where values begin to increase from 400 to 450 m/s up to values of 600 to 800 m/s is consistent with the expected depth of the top of the Memphis Sand.

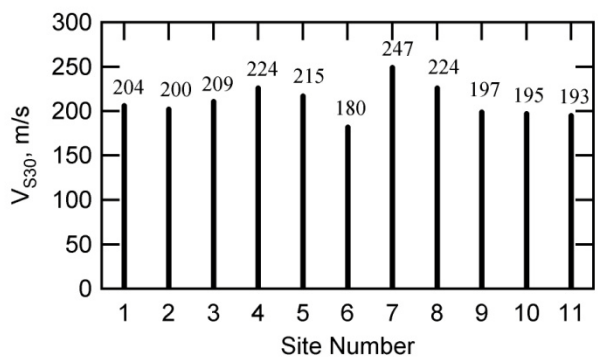

Figure 10 Average shear wave velocity values in the top 30 m, V_{S30}, at Sites 1 through 11.

Average Profile and Comparisons with Reference V_S Profiles for the Embayment

Using the eleven V_S profiles developed from this work, the arithmetic mean and standard deviation were calculated as a function of depth and compared to the reference profile developed by Romero and Rix (2001), as shown in Figure 11. A reference V_S profile for the embayment was developed by Romero and Rix (2001) from a compilation of existing V_S profiles. Also, shown in Fig. 11 is a V_S profile presented by Dorman and Smalley (1994) that was developed from p-wave well velocities. Dorman and Smalley (1994) analyzed surface waves propagating between Risco, Missouri and Memphis, Tennessee (similar extent as this study) and found the data to be consistent with the profile shown in Fig. 11. As can be observed in Fig. 7, the average profile developed from this study is in generally good agreement with the profiles developed from these previous studies.

The COV values shown in Figure 11 indicate a correlation between soil formations and V_S. In this study, the COV value was highest at the surface but fluctuated between about 0.1 to 0.2 at greater depths. It can be observed from Figures 10 and 11, that depth intervals with low COV values are consistent with depth ranges where the formation type was generally the same at each site. For example, in the depth range of 50 to 100 m, where the COV values are low (0.11 to 0.14), nearly all of the sites are in the Upper Claiborne unit. The COV values increase below this depth, as some of the sites move into the Memphis Sand formation, and then ultimately decrease again below 150 m, where all of the sites are in the Memphis Sand Formation.

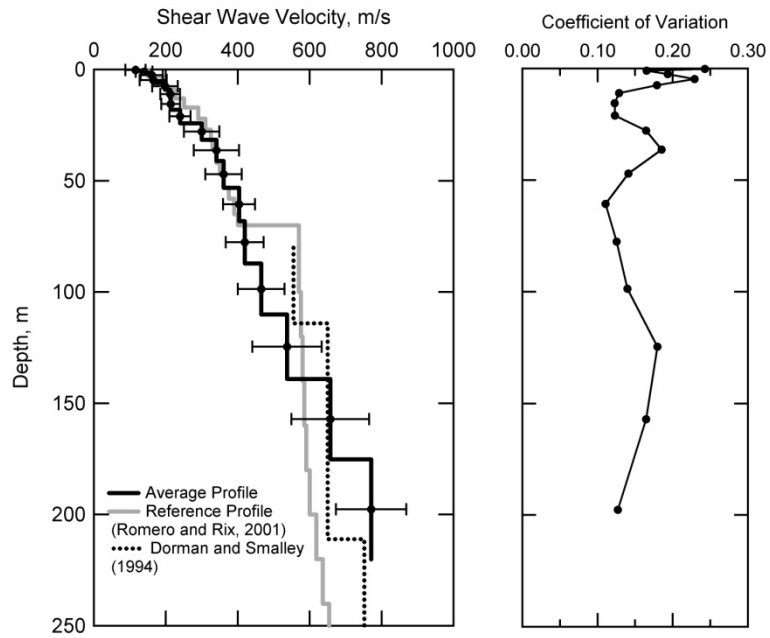

Figure 11 Average V_S profile and COV values calculated from the eleven profiles used in this study, compared with reference V_S profiles developed for the Mississippi embayment. Bars indicate ± one standard deviation.

SASW Analysis with Site Specific Profile Layering

To further investigate the relationship between shear wave velocity and soil formation, the inversion analyses were repeated using thicker layers and layer boundaries consistent with the expected change in formation type. The layering in the near-surface alluvial deposits remained unchanged, but at greater depths one or two layers were used to represent the velocities of the upper Claiborne unit and the Memphis Sand. The thicker layers were used to better estimate the average velocities of the deeper deposits. Similar fits to the experimental dispersion curves (as measured by the RMS error) were achieved using these site-specific profiles. Figure 12 shows an example comparison between the V_S profiles determined using the generic layering and site-specific profile layering for Site 10. These results illustrate one of the limitations of surface wave measurements, which is the inability to distinguish between gradual and abrupt velocity transitions at depth. However, the velocity estimates from either analysis are quite similar.

Estimation of Average Formation Velocities

Using the site-specific profiles for each site, the average V_S values for different formations were calculated. The profiles showed no measurable difference between V_S values for the Jackson, Cockfield and Cook Mountain Formations, so these formations were combined into the upper Claiborne Unit. Figure 13 shows the profiles and histograms determined for each formation/unit.

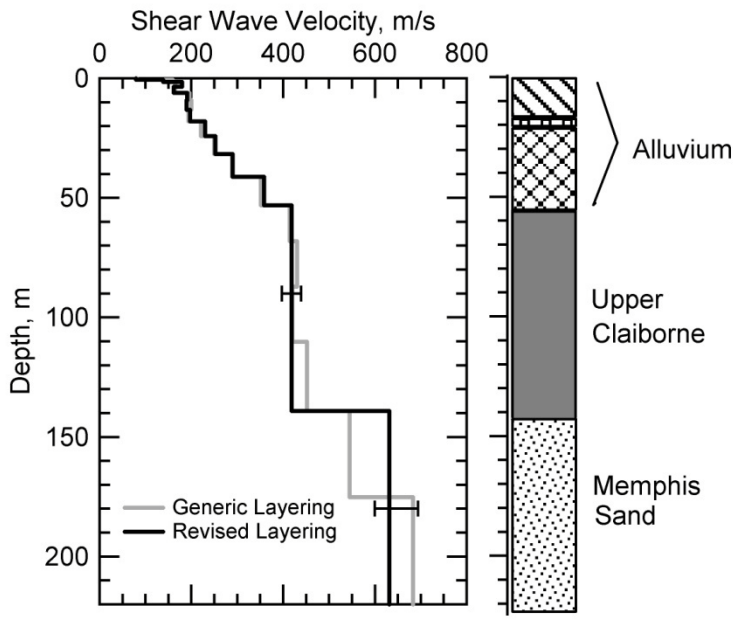

Figure 12 Comparison between V_S profiles obtained at Site 10 using the generic layering and revised site-specific layering.

The average value of 193 m/s determined for the alluvium in this study fell between the values of 171 m/s reported by Gomberg et al. (2003) and 206 m/s reported by Williams et al. (2003). The average value of 399 m/s determined from this study for the Upper Claiborne unit is also in good agreement with previous studies (about 3% lower than Gomberg et al. and 12% lower than Williams). However, the average velocity from this study of 685 m/s estimated for the Memphis Sand is notably higher than values reported by Gomberg et al. (530 m/s) or Willliams et al. (587 m/s). It should be noted that values from both the Gomberg et al. and Williams et al. studies are based primarily on shallow measurements performed in and around Memphis and are expected to yield lower velocities due to the shallower depth. Also the higher values for the Memphis Sand found in this study are consistent with well log values (600 to 800 m/s) measured in Memphis (Cramer et al., 2004). Lastly, other studies in the embayment by Street et al. (2001) and Street and Woolery (2002) report shear wave velocity values near 700 m/s at depth. One profile from Street and Wollery (2002) was within about 800 m of Site 10. Figure 14 presents a comparison of the V_S profile developed from this study to the V_S profile from Street and Woolery, 2002, and shows the consistency in the V_S values estimated at depth.

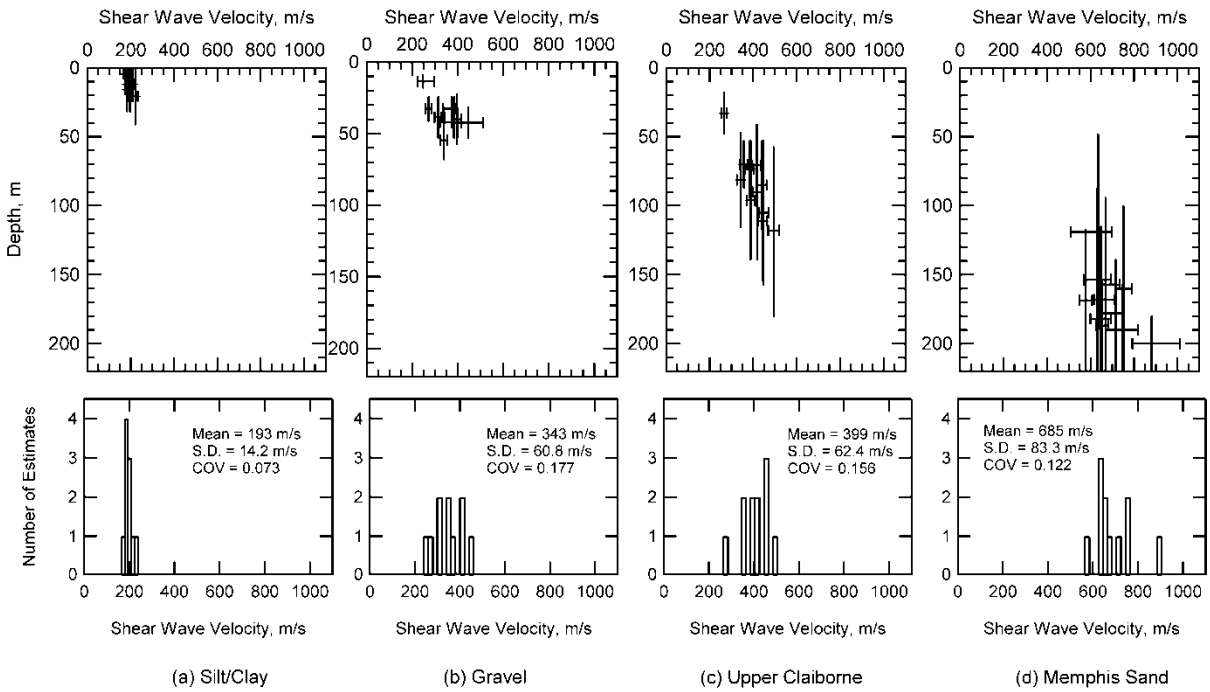

Figure 13 Results from surface wave analyses showing profiles of formation velocities and histograms of V_S values for each formation.

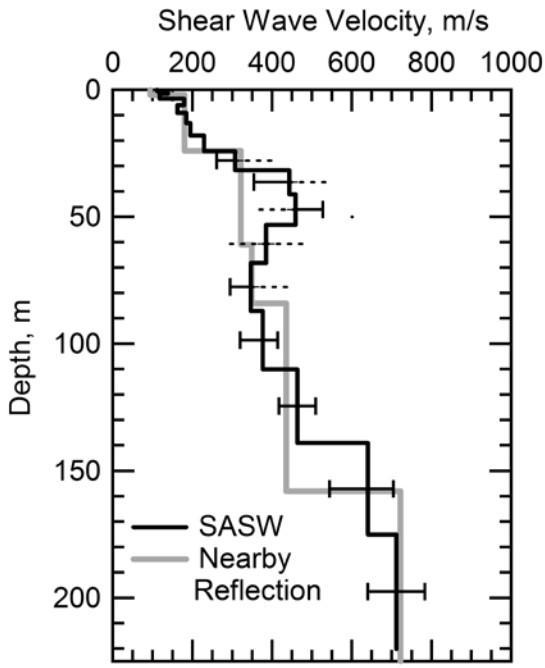

Figure 14 Comparison of V_S profiles determined at Site 10 from this study and site reported by Street and Woolery (2002) located about 800 m from Site 10.

CONCLUSIONS

The results from the analyses of the six sites measured as part of this study and the five previous deep soil profiles leads to several conclusions:

1. The low-frequency NEES vibrator used in this study was effective at generating the low-frequency energy (less than 1 Hz) needed for developing deep V_s profiles. This study was among the first application of this unique equipment to low-frequency, active-source surface wave measurements at soil sites.

2. The SASW method was shown to be a viable approach to developing deep V_s profiles. This conclusion was drawn from the observed consistency of the theoretical dispersion curves to the experimental dispersion curves, as well as the resulting V_s profiles that were consistent with the expected site conditions and V_s values from independent studies.

3. The V_s reference profile of Romero and Rix (2001) was validated by the results of this study. The average V_s profile from the eleven sites of this study was in good agreement with the profile of Romero and Rix. This is an important contribution, as this profile has been used in past site response studies of the region, but was based on very limited data for the deep soils.

4. The site-to-site variability in V_s profiles appears to be strongly related to changes in soil formation depths and thickness. The V_s profiles developed from this study showed good agreement between the depth of changes in V_s and the estimated depths to formation tops. Relationships between V_s and soil formations from this study were in good agreement with data derived from past studies.

REFERENCES

Bailey, J.P. (2008). Development of Shear Wave Velocity Profiles in the Deep Sediments of the Mississippi Embayment using Surface Wave and Spectral Ratio Methods. Ph.D. Dissertation, Department of Civil Engineering, University of Missouri, 156 pp.

Bay, J. (2003). "Shallow Shear Wave Velocity Profiling of Poorly Characterized Earthquake Site-Response Units in Urban Salt Lake Valley." NEHRP Program, USGS Award #03HQGR0049.

Brown, L.T., Boore, D.M., Stokoe II, K.H. (2000) "Comparison of shear-wave velocity profiles from SASW and downhole seismic tests at a strong-motion site," in Proc. 12th World Conference on Earthquake Engineering, Auckland, New Zealand, 30 January–4 February.

Brown, L.T., Boore, D.M., Stokoe II, K.H. (2002). "Comparison of shear-wave slowness profiles at 10 strong-motion sites from noninvasive SASW measurements and measurements made in boreholes." *Bulletin of the Seismological Society of America* 92, 3116–3133.

Chen K-C, Chiu J-M, Yang Y-T. (1994). "Qp-Qs relations in the sedimentary basin of the upper Mississippi Embayment using converted phases." *Bulletin of the Seismological Society of America*, 84(6):1861-8.

Cramer, C.H., Gomberg, J.S., Schweig, E.S., Waldron, B.A., Tucker, K. (2004). The Memphis, Shelby County, Tennessee, Seismic Hazard Maps. U.S. Geological Survey Open File Report 2004-1294., 41 pp.

Cramer, C. (2006). "Quantifying the uncertainty in site amplification modeling and its effects on site specific seismic hazard estimation in the upper Mississippi Embayment and adjacent areas." *Bulletin of Seismological Society of America* 96, 2008-2020.

Dorman, J., Smalley, R. (1994). "Low-frequency seismic surface waves in the upper Mississippi embayment." *Seismological Research Letters* 65 (2), 137-148.

Gomberg, J., Waldron, B., Schweig, E., Hwang, H., Webbers, A., Van Arsdale, R., Tucker, K., Williams, R., Street, R., Mayne, P., Stephenson, W., Odum, J., Cramer, C., Updike, R., Hutson, S., Bradley, M. (2003). "Lithology and shear velocity in Memphis, Tennessee." *Bulletin of the Seismological Society of America*, 93, 986–997.

Joh, S.H., (1996). Advances in Interpretation and Analysis techniques for Spectral-Analysis-of-Surface-Waves (SASW) Measurements. Ph.D. Dissertation, Department of Civil Engineering, University of Texas at Austin.

Kausel, E., and Roesset, J.M., (1981). "Stiffness matrices for layered soils." *Bulletion of the Seismological Society of America*, 71, 1743-1761.

Park D, Hashash YMA. (2005). “Evaluation of seismic site factors in the Mississippi Embayment. I. Estimation of dynamic properties.” *Soil Dynamics and Earthquake Engineering*, 25(2):133-44.

Parks, W.S and Carmichael, J.K. (1990). Geology and Ground-Water Resources of the Memphis Sand in Western Tennessee. U.S. Geological Survey Water Resources Investigation Report, 88-4182, 30 pp.

Rix, G., K.H. Stokoe II. (1989). “Stiffness Profiling of Pavement Subgrades.” *Transportation Research Record 1235*, TRB, National Research Council, Washington, D.C., pp. 1-9.

Romero S, and Rix G.J. (2001). Ground Motion Amplification of Soil in the Upper Mississippi Embayment, Mid-America Earthquake Center; 2001. Report No.: GIT-CEE/GEO-01-1.

Rosenblad B.L., Li J., Menq F.-Y., Stokoe K.H. (2007). “Deep Shear Wave Velocity Profiles from Surface Wave Measurements in the Mississippi Embayment.” *Earthquake Spectra*, 23(4), 791-808.

Saucier, R.T. (1994). Geomorphology and Quaternary geologic history of the lower Mississippi Valley. U.S. Army Corps of Engineers Waterways Experiment Station, 364.

Stokoe II, K.H., Nazarian, S., Rix, G.J., Sanchez-Salinero, I., Sheu, J.C., and Mok, Y.J. (1988). “In-situ seismic testing of hard-tosample soils by surface wave method.” *In* Earthquake engineering and soil dynamics. II: Recent advances in ground-motion evaluation. Edited by J.L. Von Thun. American Society of Civil Engineers, Geotechnical Special Publication 20. pp. 264–279.

Stokoe II, K.H., Wright, G.W., Bay, J.A., Roesset, J.M. (1994). “Characterization of geotechnical sites by SASW method.” *In* Geophysical Characterization of Sites, ISSMFE Technical Committee #10, edited by R.D. Woods, Oxford Publishers, New Delhi.

Stokoe KH, II, Rathje EM, Wilson CR, Rosenblad B. (2004). “Development of large-scale mobile shakers and associated instrumentation for in-situ evaluation of nonlinear characteristics and liquefaction resistance of soils.” *In* Proceedings of the 13th World Conference on Earthquake Engineering, August.

Street R, Woolery EW, Wang Z, Harris JB. (2001). “NEHRP soil classifications for estimating site-dependent seismic coefficients in the Upper Mississippi Embayment.” *Engineering Geology*, 62(1-3), 123-35.

Street R. and Woolery E.W. (2002). “Shear Wave Velocities of the Post-Paleozoic Sediments in the Upper Mississippi Embayment.” National Earthquake Hazard Reduction Program (NEHRP) Final Technical Report, United States Geological Survey, Award No. 02HQGR0023.

Van Arsdale, R.B., TenBrink, R.K. (2000). “Late Cretaceous and Cenozoic Geology of the New Madrid Seismic Zone.” *Bulletin of the Seismological Society of America*, 90, 345–356.

Williams RA, Wood S, Stephenson WJ, et al. (2003). “Surface Seismic Refraction/Reflection Measurement Determinations of Potential Site Resonances and the Areal Uniformity of NEHRP Site Class D in Memphis, Tennessee.” *Earthquake Spectra*, 19(1), 159-89.

PUBLICATIONS RESULTING FROM THIS WORK

Rosenblad, B.L., Bailey, J.P., Csontos, R., and Van Arsdale, R. “Shear Wave Velocities of Mississippi Embayment Soil Formations from Low-Frequency Surface Wave Measurements.” *Soil Dynamics and Earthquake Engineering*, (in review).

APPENDIX

SHEAR WAVE VELOCITY PROFILES USING GENERIC LAYERING

SITE 1		SITE 2		SITE 3	
Thickness (m)	S-Wave Velocity (m/s)	Thickness (m)	S-Wave Velocity (m/s)	Thickness (m)	S-Wave Velocity (m/s)
0.5	107	0.5	129	0.5	64
1	131	1	118	1	139
2	140	2	129	2	177
2.5	205	2.5	133	2.5	144
3.1	199	3.1	170	3.1	167
4	223	4	204	4	218
4.9	204	4.9	217	4.9	223
6.1	224	6.1	241	6.1	243
7.5	257	7.5	329	7.5	357
9.5	289	9.5	290	9.5	388
12	326	12	312	12	389
15	364	15	429	15	399
19	400	19	486	19	432
23	453	23	491	23	517
29	475	29	427	29	688
36	527	36	643	36	866
45	603	H.S.	735	H.S.	910
H.S.	742				

SITE 4		SITE 5		SITE 6	
Thickness (m)	S-Wave Velocity (m/s)	Thickness (m)	S-Wave Velocity (m/s)	Thickness (m)	S-Wave Velocity (m/s)
0.5	127	1	108	0.5	108
1	135	1	131	1	120
2	190	1	185	2	142
2.5	237	3	179	2.5	123
3.1	208	3	234	3.1	171
4	219	3	252	4	182
4.9	221	6	246	4.9	192
6.1	222	6	218	6.1	209
7.5	279	6	255	7.5	241
9.5	301	6	264	9.5	327
12	301	12	316	12	386
15	496	12	448	15	418
19	409	25	531	19	417
23	429	25	611	23	421
29	576	50	713	29	478
36	716	H.S.	822	36	621
H.S.	905			H.S.	750

SITE 7		SITE 8		SITE 9	
Thickness (m)	S-Wave Velocity (m/s)	Thickness (m)	S-Wave Velocity (m/s)	Thickness (m)	S-Wave Velocity (m/s)
0.5	171	0.5	109	0.5	81
1	166	1	191	1	153
2	220	2	166	2	167
2.5	114	2.5	142	2.5	163
3.1	265	3.1	239	3.1	191
4	258	4	222	4	194
4.9	271	4.9	187	4.9	192
6.1	309	6.1	278	6.1	226
7.5	332	7.5	395	7.5	254
9.5	333	9.5	439	9.5	290
12	320	12	397	12	347
15	329	15	374	15	411
19	356	19	409	19	424
23	412	23	488	23	419
29	487	29	552	29	455
36	579	36	584	36	548
H.S.	755	H.S.	850	H.S.	683

SITE 10		SITE 11	
Thickness (m)	S-Wave Velocity (m/s)	Thickness (m)	S-Wave Velocity (m/s)
0.5	111	0.5	131
1	138	1	113
2	118	2	133
2.5	179	2.5	190
3.1	162	3.1	164
4	184	4	175
4.9	194	4.9	197
6.1	229	6.1	231
7.5	307	7.5	290
9.5	443	9.5	384
12	459	12	412
15	385	15	390
19	346	19	399
23	376	23	494
29	463	29	594
36	640	36	685
H.S.	712	H.S.	807